Carbohydrate Polymers 95 (2013) 773–779

Contents lists available at SciVerse ScienceDirect

Carbohydrate Polymers

journal homepage: www.elsevier.com/locate/carbpol

Effect of cellulose whisker content on the properties of poly(ethylene-co-vinyl acetate)/cellulose composites

Silviya Elanthikkal[a], Unnikrishnan Gopalakrishnapanicker[a,*], Soney Varghese[b], James T. Guthrie[c], Tania Francis[d]

[a] Department of Chemistry, National Institute of Technology Calicut, 673601, India
[b] School of Nanoscience and Technology, National Institute of Technology Calicut, 673601, India
[c] Department of Colour Science, School of Chemistry, University of Leeds, LS2 9JT, UK
[d] St. Joseph's College Devagiri, Calicut, Kerala 673008, India

ARTICLE INFO

Article history:
Received 25 October 2012
Received in revised form 23 January 2013
Accepted 21 February 2013
Available online 4 March 2013

Keywords:
Polymer composites
Cellulose whiskers
Tensile properties

ABSTRACT

The reinforcing effect of cellulose whiskers, produced from banana waste fibres, has been investigated using poly(ethylene-co-vinyl acetate) [EVA]/cellulose whisker composites. Cellulose whiskers, approximately 300 nm long and 30 nm wide, were obtained via a sulphuric acid hydrolysis method. The effects of the cellulose whisker loading on the thermal properties, mechanical properties and on the morphological features of the composites have been investigated. EVA copolymer with a vinyl acetate segment content of 40% has been used for composite fabrication. The developed composites showed superior thermal and mechanical properties relative to that of the EVA copolymer alone. Three theoretical models, namely the Halpin–Tsai model, the Kerner model and the Nicolais–Narkis model have been employed to provide a basis for the comparison of the results with the observations from the tensile investigations.

1. Introduction

The modification of synthetic macromolecules with biomacromolecules has by now gained significant attention because of the possibility for the development of a spectrum of products through environmentally friendly strategies (Ljungberg, Cavaille, & Heux, 2006; Samir, Alloin, & Dufresne, 2005; Sanchez-Garcia, Gimenez, & Lagaron, 2008; Saxena & Ragauskas, 2009; Wu, Henriksson, Liu, & Berglund, 2007). Poly(ethylene-co-vinyl acetate) [EVA], is a widely used polymer, with a variety of industrial applications (Henderson, 1993). The copolymer contains relatively polar vinyl acetate repeat units and non-polar ethylene units. As the vinyl acetate content increases, the copolymer becomes less crystalline and more polar. By varying the vinyl acetate content, EVA-based copolymers can be tailored towards applications as rubbers, thermoplastic elastomers and plastics used for various applications such as packaging films, adhesives/paper coatings, wire and cable insulation, and barrier sheets (Yin, Zhang, & Yao, 2006).

An interesting observation in this regard is that only a few reports are available on the modification of EVA with cellulosic fibres. Mydul, Ahmed, Haque, Gafur, and Kabir (2009) studied the mechanical properties of EVA/cellulose acetate [CA]-containing natural fibres (*Sterculia villosa*). They observed that the tensile strength of EVA composites decreased with the addition of fibres whereas, in CA composites, the tensile strength increased due to a better distribution of fibres. Malunka, Luyt, and Krump (2006) have prepared EVA/sisal fibre composites using melt mixing with dicumyl peroxide [DCP] as a free radical initiator. They highlighted the fact that through using DCP as the initiator, grafting between EVA and sisal fibre took place. These composites were thermally more stable than either the EVA block copolymer or the sisal fibre alone. Dikobe and Luyt (2009) examined composites of PP/EVA blends with wood powder [WP] and reported that the WP influenced the crystallization behaviour of EVA. Espert, Vilaplana, and Karlsson (2004) studied PP/EVA/Technocel 165 [Cell] composites and reported that EVA improved the resistance of the composites to water absorption. EVA block copolymers also offer the possibility of preparing compatible blends with biodegradable polymers, such as poly(lactic acid) [PLA]. Such composites could be advantageously exploited for the preparation of composites that contain natural fillers.

Chauve, Heux, Arouini, and Mazeau (2005) carried out a molecular modelling examination of the reinforcing effect of cellulose whiskers in EVA copolymer matrices with different vinyl acetate segment contents. The reinforcing effect increased with increase

* Corresponding author. Tel.: +91 495 2285302; fax: +91 495 2287250.
E-mail addresses: silviyaek@gmail.com, slvyek@yahoo.co.in (S. Elanthikkal), unnig@nitc.ac.in (U. Gopalakrishnapanicker).

0144-8617/$ – see front matter © 2013 Elsevier Ltd. All rights reserved.
http://dx.doi.org/10.1016/j.carbpol.2013.02.039

in the vinyl acetate segment content of the copolymer. However, levelling off in properties was observed with greater acetate segment contents that were above 40 wt% of vinyl acetate. Related modelling studies suggested the existence of hydrogen bonding between the carbonyl groups of the matrix and the hydroxyl groups of the cellulose whiskers at the interface. The authors proposed that such interactions might be complicated in a copolymer blend that had an increased vinyl acetate segment content. This would be due to the steric hindrance that would be induced by the acetate segments. Thus, to be fully effective, the number of possible hydrogen bonding interactions needs to be a compromise brought about by the total number of vinyl acetate segments and the ability of these segments/groups to become engaged with hydroxyl partners at the cellulose whisker surfaces.

No systematic study has yet been reported on the utilization of cellulose whiskers derived from banana waste fibre for the reinforcement of EVA. The present article highlights the results of a detailed investigation on the composites of EVA and cellulose whiskers derived from pseudo-stem of banana plant.

2. Experimental

2.1. Materials

EVA copolymer, having a vinyl acetate segment content of 40% (EVAFLEX), was supplied by Dupont Mitsui Polychemicals Co. Ltd., Tokyo, Japan. The banana fibres were supplied by the Fibre Design Centre, Khadi and Village Industries Commission (KVIC), Trivandrum, India. The NaOH and the NaOCl which were used for the pre-treatment of banana fibres, were of analytical purity. Sulphuric acid (>98%) was obtained from Fisher Scientific, UK. Tetrahydrofuran [THF] was purchased from Sigma Aldrich, UK.

2.2. Isolation of cellulose whiskers from banana fibres

The cellulose whiskers were generated from the banana fibres by an acid catalyzed hydrolysis. Initially, the ground banana fibres were screened using a test sieve of 150 μm aperture size (Endecotts Ltd., England). The screened fibres were subjected to an alkaline treatment and bleaching prior to acid hydrolysis. The pretreated banana fibres were then treated with a 64 wt% sulphuric acid solution at 45 °C for 4 h. The aqueous suspension of the cellulose whiskers that was obtained after dialysis and ultrasonication, was freeze dried (LSL Secfroid, Switzerland). A detailed procedure for the isolation of cellulose from banana fibres, using different reaction conditions, is available elsewhere (Silviya, Unnikrishnan, Varghese, & Guthrie, 2010).

2.3. Preparation of EVA/cellulose composite membranes

For the fabrication of EVA40 copolymer/cellulose whisker composite films, 3 g EVA40 was dissolved in 50 g of THF, with stirring overnight at room temperature. In a parallel exercise, a dispersion of the cellulose whiskers in THF was prepared by separately weighing a known amount of the freeze dried cellulose whiskers. Dispersions with different wt% (2.5%, 5%, 7.5% and 10%) of cellulose whiskers in THF were well mixed with the EVA copolymer-THF solution. Each of these dispersions was cast onto glass plates (17 cm × 17 cm × 0.5 cm) and dried at room temperature in a fume cupboard. The formulations used in the composite preparations are given in Table 1.

Table 1
Formulation of EVA40/cellulose composite membranes.

Sample code	EVA40 (g)	Cellulose (wt%)
EVA40	3	0
EVA40A	3	2.5
EVA40B	3	5.0
EVA40C	3	7.5
EVA40D	3	10

2.4. Characterization

2.4.1. FT-IR spectroscopic analysis

The composite films were examined by FT-IR spectroscopy, over the wavenumber range of 400–4000 cm^{-1}, using a Perkin-Elmer Spectrum One spectrophotometer.

2.4.2. Morphology studies

The morphology of the composite films was investigated by scanning electron microscopy (SEM). Prior to evaluation by SEM, the samples were sputter coated with gold to avoid subsequent charging during SEM analysis. Images were taken using a JEOL JSM – 820 model SEM.

2.4.3. Thermal analysis

EVA/cellulose composite films were analyzed by thermogravimentric analysis (TGA), and by differential scanning calorimetry (DSC). A TGA 2050 series thermogravimetric analyzer (TA Instruments) was used, across a temperature range from 30 °C to 500 °C at a heating rate of 10 °C/min in a nitrogen environment. The melting temperature of each sample was recorded using a Differential Scanning Calorimeter (DSC 2010 series, TA Instruments) from −50 °C to 150 °C with a heating rate of 10 °C/min.

2.4.4. Mechanical properties evaluation

The mechanical properties of the composite films were determined using a Universal Testing Machine (Instron Corp., Canton, MA, USA), following the ASTM D 882-88 protocol. The initial grip separation and the crosshead speed were set at 40 mm and 50 mm/min, respectively. Tensile strength, strain at break and elastic modulus of the composites were obtained. The data reported are the mean of at least five experiments.

3. Results and discussion

3.1. Characteristics of cellulose whiskers

The detailed characterization of the cellulose whiskers that were produced from waste banana fibres has been described previously (Silviya et al., 2010). The TEM analysis of cellulose whiskers showed that the whiskers have an average aspect ratio of 10 (Silviya, Unnikrishnan, Francis, Varghese, & Guthrie, 2012). From XRD analysis, the crystallinity index of cellulose whiskers was found to be 70.20%. Average molecular weight and density of cellulose whiskers were 12,960 g/mol and 1350 kg/m^3, respectively.

3.2. FT-IR spectroscopic analysis

Fig. 1 gives the FT-IR spectra of the cellulose whiskers, of the "pure" EVA40 copolymer and of the EVA40 copolymer/cellulose whisker composites. The typical absorption bands of the vinyl acetate group appear at 1736, 1234, and 1015 cm^{-1}, while the absorption bands being ascribed to ethylene group are present at 2919, 2854, 1469, 1374, and 720 cm^{-1}. The peaks at 2916 cm^{-1} and 2854 cm^{-1} in the spectra of EVA samples have been attributed to the asymmetric and symmetric vibrations respectively of aliphatic

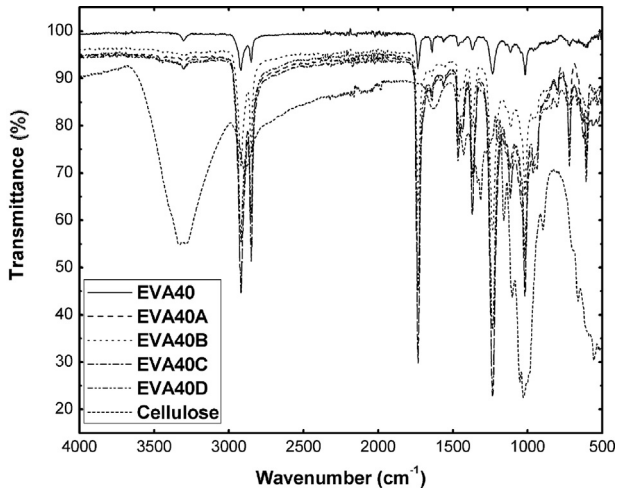

Fig. 1. FT-IR spectra of the cellulose whiskers, of the EVA40 copolymer and of the EVA40/cellulose whisker composites.

groups $(—CH_2—)_n$. The 1736 cm^{-1} peak corresponds to carbonyl stretching vibrations of acetate groups in EVA. The addition of cellulose into the EVA40 matrix enhances the width and intensity of the peaks at 3600–3000 cm^{-1} (—O—H vibration in cellulose) and 1022 cm^{-1} (—C—O—C— pyranose ring skeletal vibration in cellulose). For the EVA40/cellulose whisker composites, the typical absorption bands of the vinyl acetate segments/groups experience small shifts from 1736.6, 1234.1, and 1015.5 cm^{-1} to 1733.9, 1235.9 and 1017.8 cm^{-1}, respectively. The band shifts clearly show that there are interactions between the hydroxyl groups on the surface of cellulose and the relatively polar vinyl acetate segments/groups of the EVA copolymer component.

3.3. Morphology studies

Fig. 2(a)–(e) gives the SEM images of the EVA40 copolymer and of the EVA40/cellulose whisker composites. From the images, it is clear that the cellulose particles are well dispersed and properly wetted by the matrix. The filler appears to be more or less evenly distributed within the polymeric matrix, up to a 7.5 wt% of cellulose whisker loading. At greater percentage of cellulose whiskers, the distance between the cellulose whiskers decreases leading to agglomerated phases within the matrix. The aggregates can be seen in the image of the composite that contained 10 wt% of cellulose whiskers.

3.4. Thermal analysis

Fig. 3(a) gives the TGA thermograms of the cellulose whisker, of the EVA40 copolymer and of the EVA40/cellulose whisker composites. As with the EVA40 copolymer, the EVA40/cellulose composites gave two step degradation profiles. The onset degradation temperature and maximum degradation temperature of the composites were determined from DTG (differential thermogravimetric) evaluations. The values obtained are given in Table 2. The onset temperature of degradation and the DTG peak temperature of the EVA40/cellulose composites were higher than those of the "pure" components (cellulose whisker and EVA40) for both peaks. However, the DTG peak temperatures of the composites were very similar, irrespective of their cellulose whisker content.

Table 3
DSC data of the EVA40 copolymer and of the EVA40/cellulose whisker composites.

Samples	Tm_1 (°C)	Tm_2 (°C)	Tm_3 (°C)	Tg (°C)	ΔH_m (J g^{-1})	X_c (%)
EVA40	9.2	34.4	50.9	−36.8	19.9	6.8
EVA40A	11.7	34.0	45.7	−37.5	20.2	6.9
EVA40B	15.7	36.2	48.1	−39.2	20.8	7.1
EVA40C	11.7	36.8	53.2	−36.1	24.6	8.4
EVA40D	14.3	36.5	54.1	–	23.7	8.1

The DSC traces that were obtained for the EVA40 copolymer and for EVA40/cellulose whisker composites are shown in Fig. 3(b). Amorphous and crystalline materials can be differentiated by the use of a plot of the enthalpy associated with phase changes as a function of increasing temperature. Crystalline materials show sharp endothermic melting peaks. The DSC patterns for the EVA40 copolymer and for EVA40/cellulose whisker composites give three endothermic peaks. These peaks are due to the melting of the crystalline ethylene segments and the amorphous vinyl acetate segments. The complex amorphous nature of EVA consists of an interfacial (less mobile) phase and a more melt-like (more mobile) amorphous phase (Almeida et al., 2011).

The values of heat of fusion can provide important information concerning the crystallinity of the composites. The degree of crystallinity (X_c) of the composites was calculated from the heat of fusion (ΔH_m), obtained from the area under the three endothermic peaks of each sample. The value 293 J g^{-1} was used for the heat of fusion of 100% crystalline EVA. This choice was made on the basis that polyethylene is stated to have a ΔH_m° value of 293 J g^{-1} (Wang et al., 2011). The crystallinity index values (X_c (%)) were calculated using Eq. (1) (Almeida et al., 2011).

$$X_c(\%) = \frac{\Delta H_m}{\Delta H_m^\circ} \times 100 \quad (1)$$

The melting temperatures and the calculated crystallinity values are presented in Table 3.

3.5. Mechanical properties

Fig. 4(a)–(c) shows the effect of the cellulose content on the tensile strength, the percentage strain at break and the elastic modulus of the EVA40/cellulose whisker composites. The tensile strength of the composites increases with the initial increase in the cellulose whisker content. However, when the cellulose whisker content was increased beyond 7.5 wt%, a decrease in the tensile strength was observed. At greater cellulose whisker loadings, cellulose–cellulose interactions become more dominant than the cellulose–matrix

Table 2
DTG data for the EVA40 copolymer and for the EVA40/cellulose whisker composites.

Samples	First degradation		Second degradation	
	Onset temperature of degradation (°C)	DTG peak temperature (°C)	Onset temperature of degradation (°C)	DTG peak temperature (°C)
Cellulose	230	326	410	443
EVA40	273	341	399	463
EVA40A	285	353	403	470
EVA40B	286	354	403	469
EVA40C	287	356	404	469
EVA40D	288	356	404	470

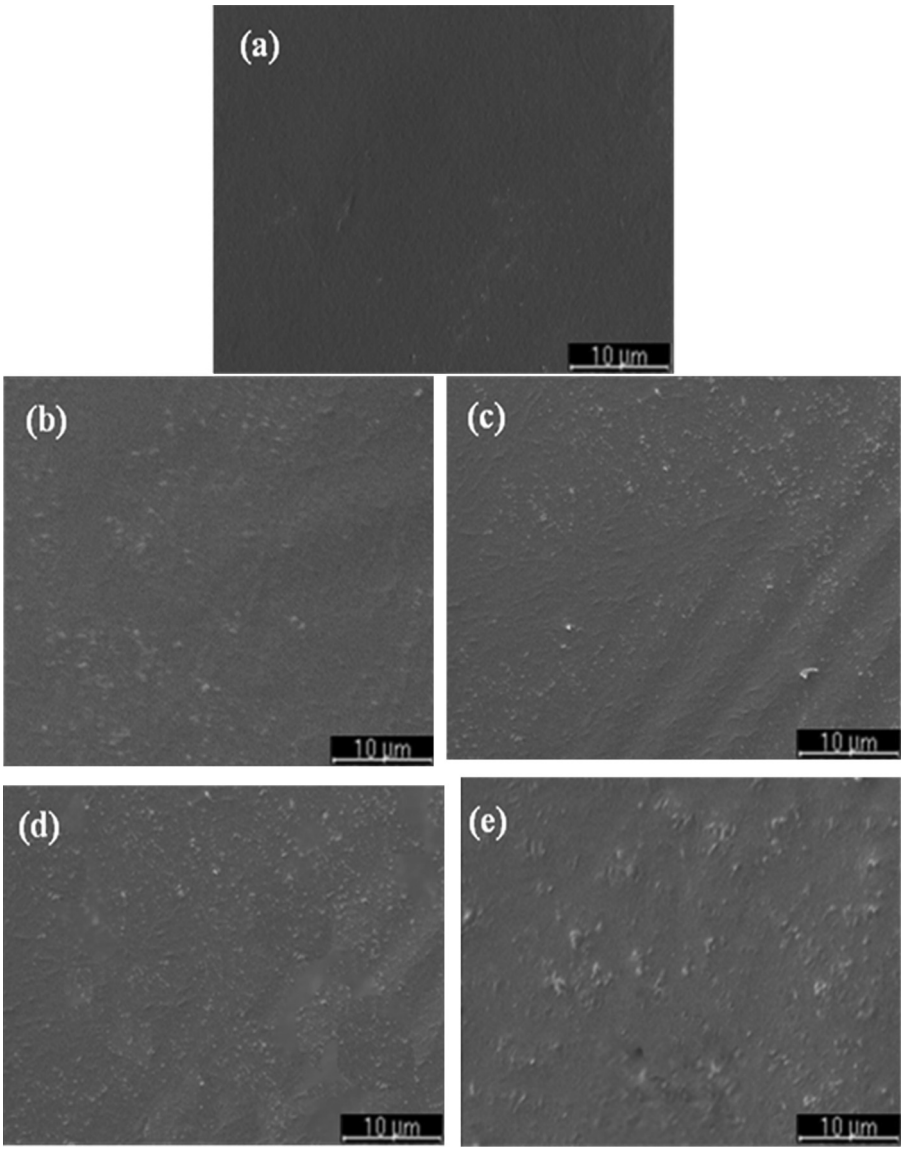

Fig. 2. SEM images of: (a) EVA40, (b) EVA40/2.5 wt% cellulose, (c) EVA40/5 wt% cellulose, (d) EVA40/7.5 wt% cellulose and (e) EVA40/10 wt% cellulose composites.

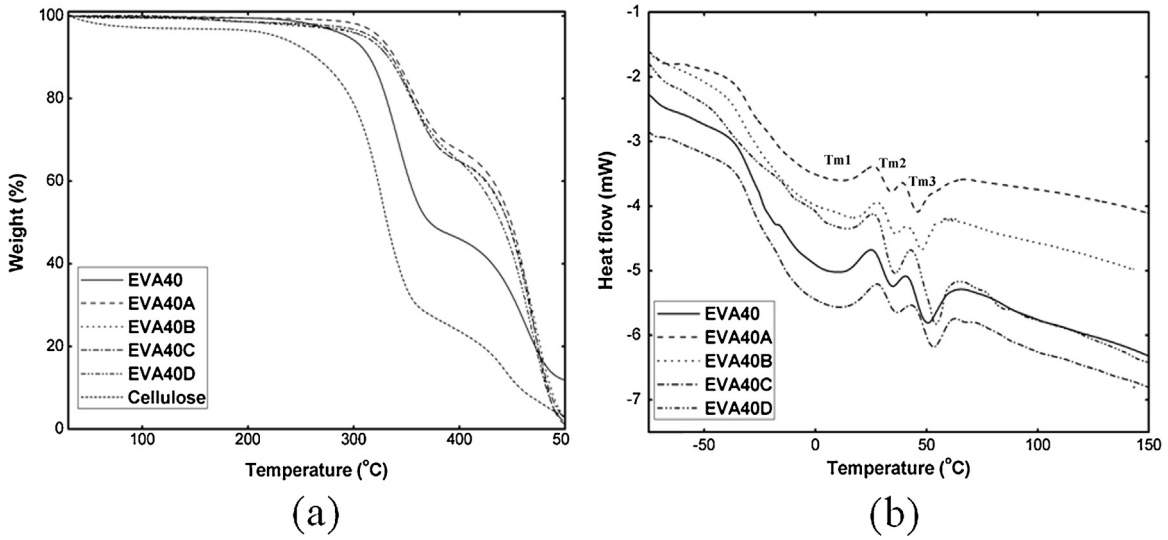

Fig. 3. (a) Thermogravimetric analytical decomposition profiles for the cellulose whisker, for the EVA40 copolymer and for the EVA40/cellulose whisker composites. (b) DSC patterns of the EVA40 copolymer and of the EVA40/cellulose whisker composites.

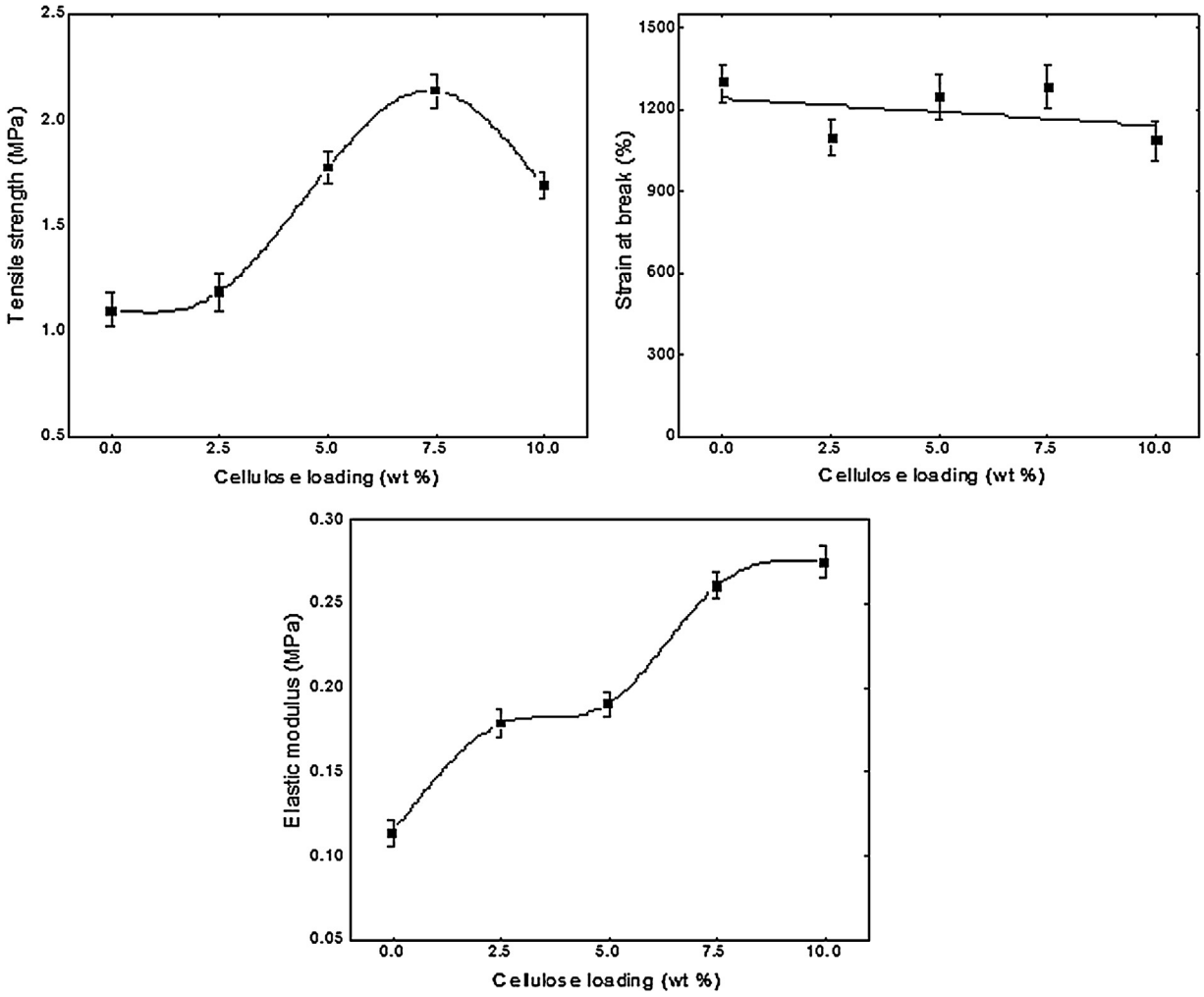

Fig. 4. Effect of cellulose whisker loading on: (a) the tensile strength, (b) the strain at break and (c) the elastic modulus of EVA40/cellulose whisker composites.

interactions. The elastic modulus of the composites increased with increase in the cellulose whisker content because of the stiffness of the cellulose whiskers. However, the percentage strain at break of the composites did not change markedly with increase in the cellulose whisker content. This effect is probably due to the compensating nature of the more elastic EVA40.

3.6. Comparison of the mechanical properties with theoretical model predictions

To gain a better understanding of the interactions that might be taking place between the dispersed phase (cellulose whiskers) and the matrix (EVA copolymer), the tensile test data were analyzed using prediction models/theories.

3.6.1. Relative tensile strength (RTS)

Relative tensile strength is the ratio of the tensile strength of the composite to the tensile strength of the pure matrix. Two theoretical models were used to predict the tensile strength of EVA/cellulose whisker composites. The first is the Nicolais and Narkis model (Nicolais & Narkis, 1971), given as Eq. (2).

In this model, the relative tensile strength RTS is given by:

$$\mathrm{RTS} = \frac{\sigma_c}{\sigma_{EVA}} = 1 - 1.20\phi_f^{2/3} \quad (2)$$

In Eq. (2), σ_c and σ_{EVA} are the tensile strength of the composite and of the neat EVA copolymer, respectively. ϕ_f is the volume fraction of the filler in the matrix. Use of this model assumes that there is no adhesion between the filler and the matrix.

The second model is the Halpin–Tsai model (Halpin & Kardos, 1976), represented by Eq. (3).

$$\mathrm{RTS} = \frac{\sigma_c}{\sigma_{EVA}} = \frac{1 + \zeta\eta_T\phi_f}{1 - \eta_T\phi_f} \quad (3)$$

η_T is given by Eq. (4):

$$\eta_T = \frac{R_T - 1}{R_T + \zeta} \quad (4)$$

Here, R_T is the ratio of filler tensile strength to that of neat EVA. ζ, as used in Eqs. (3) and (4), is the aspect ratio (=10) and ϕ_f is the volume fraction of the filler in the matrix.

Fig. 5(a) gives a comparison of the experimental RTS values with the RTS values calculated on the basis of the use of the Halpin–Tsai equation and the Nicolais–Narkis equation, for various filler loadings. The experimental results better matches with the Halpin–Tsai prediction than the Nicolais–Narkis prediction. The Halpin–Tsai model assumes that there is perfect interaction between the filler and the matrix. The agreement of the results with Halpin–Tsai model would suggest the existence of significant interaction between the cellulose whiskers and the EVA copolymer, i.e., polar–polar interaction. The experimental results are not in agreement with the prediction based on the use of the Nicolais–Narkis model. The percentage deviation of experimental RTS values from the theoretical prediction by the Nicolais–Narkis model was very

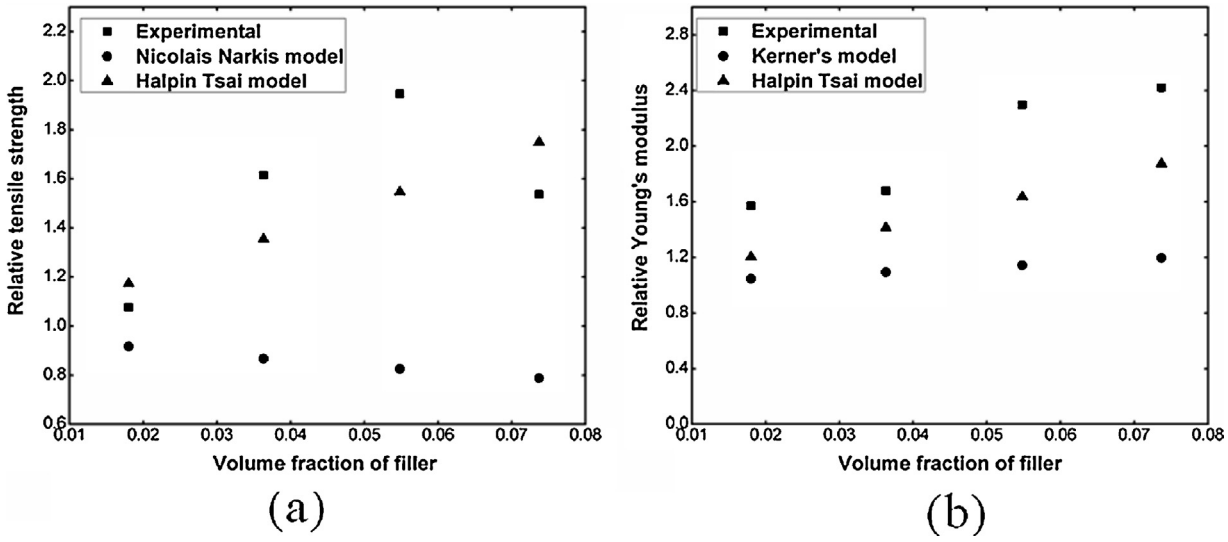

Fig. 5. (a) Comparison of experimental RTS values of EVA40/cellulose whisker composites with values of the theoretical models. (b) Comparison of experimental RYM values of the EVA40/cellulose whisker composites with values of the theoretical models.

large compared to the result by Halpin–Tsai model. This is because Nicolais–Narkis model assumes no interaction between the filler and the matrix.

3.6.2. Relative Young's modulus (RYM)

Relative Young's modulus is the ratio of the Young's modulus of the composite to the Young's modulus of the pure matrix. Two theoretical models have been used in an attempt to explain the experimental Young's modulus values that were obtained for the EVA/cellulose whisker composites. The first is Kerner's model (Kerner, 1956), represented by Eq. (5).

$$\mathrm{RYM} = \frac{E_c}{E_{EVA}} = 1 + \left(\frac{\phi_f}{1-\phi_f}\right)\left(\frac{15(1-\nu)}{8-10\nu}\right) \quad (5)$$

In Eq. (5), E_c and E_{EVA} are the Young's moduli of composite and pure EVA, respectively. ν is the Poisson's ratio of the "pure" EVA copolymer, taken as 0.49 (Miura, Maeda, Machi, & Matsuda, 2007). The model assumes the presence of poor adhesion between the filler and its matrix.

The second model to be applied was the Halpin–Tsai model (Halpin & Kardos, 1976). This model predicts the elastic constants of composite materials as a function of the aspect ratio of the filler, when the constituent properties and the volume fractions of the two phases (matrix and reinforcement) are known. The form of the Halpin–Tsai equation (as Eq. (6)), which is complementary to Eq. (3), can be written as:

$$\mathrm{RYM} = \frac{E_c}{E_{EVA}} = \frac{1+\zeta\eta_E\phi_f}{1-\eta_E\phi_f} \quad (6)$$

Here, E_c and E_{EVA} are the Young's modulus of the composite and the matrix respectively; ϕ_f is the filler volume fraction and ζ is the aspect ratio. η_E is given by Eq. (7).

$$\eta_E = \frac{R_E - 1}{R_E + \zeta} \quad (7)$$

In Eq. (7), R_E is the ratio of the modulus of the filler to the modulus of the matrix.

Fig. 5(b) shows the variation of the relative Young's modulus (RYM) with the volume fraction of the filler in the composites. The experimental RYM values were compared with the RYM values obtained by using Halpin–Tsai model and Kerner's model. As the volume fraction of cellulose whiskers increases, the RYM value progressively increases due to the stiffening effect of cellulose whisker chains. The Halpin–Tsai model assumes the existence of perfect adhesion between the filler and its matrix. The RYM experimental results that were obtained in this study are interestingly closer to the Halpin–Tsai model, as was found for the RTS values. As the Kerner's model assumes little interaction between the filler and the matrix, the experimental RYM values of the composites showed larger deviation from the Kerner's prediction compared to the result by Halpin–Tsai model.

4. Conclusions

New composite materials based on poly(ethylene-co-vinyl acetate) and cellulose whiskers have been prepared and characterized by different techniques. The improved mechanical properties of the EVA40/cellulose whisker composites with increasing whisker content have been attributed to the good distribution of the cellulose whiskers in the EVA40 copolymer matrix and due to the polar–polar interaction between the cellulose whiskers and EVA40 matrix. The results obtained from the mechanical tests of the EVA/cellulose whisker composites were compared with the theoretical predictions using the Halpin–Tsai, the Nicolais–Narkis and the Kerner's model. The experimental results showed better agreement with the prediction given by the use of the Halpin Tsai model. This model assumes that there is perfect wetting of the filler by the matrix.

Acknowledgements

The authors acknowledge the UK-India Education Research Initiative programme (UKIERI) for the financial support that was provided during this investigation. The last author thanks the Department of Science and Technology, Govt. of India for the fellowship under the SERC-FAST Track Scheme for Young Scientist.

References

Almeida, A., Possemiers, S., Boone, M. N., De Beer, T., Quinten, T., Van Hoorebeke, L., et al. (2011). Ethylene vinyl acetate as matrix for oral sustained release dosage forms produced via hot-melt extrusion. *European Journal of Pharmaceutics and Biopharmaceutics*, *77*, 297–305.

Chauve, G., Heux, L., Arouini, R., & Mazeau, K. (2005). Cellulose poly(ethylene-co-vinyl acetate) nanocomposites studied by molecular modeling and mechanical spectroscopy. *Biomacromolecules*, *6*, 2025–2031.

Dikobe, D. G., & Luyt, A. S. (2009). Morphology and properties of polypropylene/ethylene vinyl acetate copolymer/wood powder blend composites. *eXPRESS Polymer Letters*, *3*, 190–199.

Espert, A., Vilaplana, F., & Karlsson, S. (2004). Comparison of water absorption in natural cellulosic fibres from wood and one-year crops in polypropylene composites and its influence on their mechanical properties. *Composites Part A: Applied Science and Manufacturing*, *35*, 1267–1276.

Halpin, J. C., & Kardos, J. L. (1976). Halpin–Tsai equations: A review. *Polymer Engineering and Science*, *16*, 344–352.

Henderson, A. M. (1993). Ethylene-vinyl acetate (EVA) copolymers: A general review. *Electrical Insulation Magazine, IEEE*, *9*, 30–38.

Kerner, E. H. (1956). The elastic and thermo-elastic properties of composite media. *Proceedings of the Physical Society London*, *69*, 808–813.

Ljungberg, N., Cavaille, J. Y., & Heux, L. (2006). Nanocomposites of isotactic polypropylene reinforced with rod-like cellulose whiskers. *Polymer*, *47*, 6285–6292.

Malunka, M. E., Luyt, A. S., & Krump, H. (2006). Preparation and characterization of EVA–sisal fibre composites. *Journal of Applied Polymer Science*, *100*, 1607–1617.

Miura, J., Maeda, Y., Machi, H., & Matsuda, S. (2007). Mouth guards: Difference in longitudinal dimensional stability between single- and double-laminated fabrication techniques. *Dental Traumatology*, *23*, 9–13.

Mydul, M. A., Ahmed, T., Haque, M. M., Gafur, M. A., & Kabir, H. A. N. M. (2009). Mechanical properties of natural fibre containing polymer composites. *Polymer-Plastic Technology and Engineering*, *48*, 110–113.

Nicolais, L., & Narkis, M. (1971). Stress–strain behavior of styrene-acrylonitrile/glass bead composites in the glassy region. *Polymer Engineering and Science*, *11*(3), 194–199.

Samir, M. A. S. A., Alloin, F., & Dufresne, A. (2005). Review of recent research into cellulosic whiskers, their properties and their application in nanocomposite field. *Biomacromolecules*, *6*, 612–626.

Sanchez-Garcia, M. D., Gimenez, E., & Lagaron, J. M. (2008). Morphology and barrier properties of solvent cast composites of thermoplastic biopolymers and purified cellulose fiber. *Carbohydrate Polymers*, *71*, 235–244.

Saxena, A., & Ragauskas, A. J. (2009). Water transmission barrier properties of biodegradable films based on cellulosic whiskers and xylan. *Carbohydrate Polymers*, *78*, 357–360.

Silviya, E. K., Unnikrishnan, G., Francis, T., Varghese, S., & Guthrie, J. T. (2012). Barrier properties of poly(ethylene-co-vinyl acetate)/cellulose composite membranes. *Polymer Engineering and Science*, *52*, 2140–2146.

Silviya, E. K., Unnikrishnan, G., Varghese, S., & Guthrie, J. T. (2010). Cellulose microfibres produced from banana plant wastes: Isolation and characterization. *Carbohydrate Polymers*, *80*, 852–859.

Wang, Y., Zhang, L., Zhou, S., Huang, D., Gao, S., Gong, M., et al. (2011). Influence of processing condition and HA content on the crystallization behavior of HA-filled EVA biocomposites. *Polymer Engineering and Science*, *51*, 341–346.

Wu, Q. J., Henriksson, M., Liu, X., & Berglund, L. A. (2007). A high strength nanocomposite based on microcrystalline cellulose and polyurethane. *Biomacromolecules*, *8*, 3687–3692.

Yin, J., Zhang, J., & Yao, Y. (2006). Melt grafting of poly(ethylene-vinyl acetate) copolymer with maleic anhydride. *Journal of Applied Polymer Science*, *102*, 841–846.